



**Mondragon** Biblioteka  
**Unibertsitatea** Biblioteka

biblioteka@mondragon.edu

This is a preprint version of the following article, accepted for publication in:

Daniel Soler, Thomas H. C. Childs & Pedro Jose Arrazola (2015) A Note on Interpreting Tool Temperature Measurements from Thermography, *Machining Science and Technology*, 19:1, 174-181, DOI: [10.1080/10910344.2014.991027](https://doi.org/10.1080/10910344.2014.991027)

# A NOTE ON INTERPRETING TOOL TEMPERATURE MEASUREMENTS FROM THERMOGRAPHY

Short title: Interpreting tool temperature measurements

D. Soler<sup>1\*</sup>, T.H.C.Childs<sup>2</sup> and P.J. Arrazola<sup>1</sup>

<sup>1</sup> Manufacturing Department, Faculty of Engineering, Mondragon University, Mondragon, Spain

<sup>2</sup> School of Mechanical Engineering, University of Leeds, Leeds, UK

\*Corresponding author: email address: dsoler@mondragon.edu

Abstract: Thermography (thermal imaging) is a well-established experimental method for studying cutting tool temperature distributions. In one form cutting edge temperatures within the chip / tool contact area are deduced from thermal images of tool faces normal to the cutting edge but offset from the contact region. In general practice, the offset is made as small as possible ( $\ll 1$  mm) and it is assumed that the observed temperature is the same as that within the contact. In this short communication an approximate analytical model is developed for the influence of the offset on the observed temperature. The predictions from the model are compared with previously unpublished existing results on the machining of Ti alloys (Ti6Al4V and Ti5Al4V) and on steel (AISI 4140). It is shown that ignoring the offset may introduce underestimates of cutting edge temperature of  $\approx 30\%$  or more. This is large compared to the usually considered uncertainties of  $\pm 5\%$  from camera and tool emissivity calibration. There is a need for a dedicated study of this effect.

Key words: Metal machining, Temperature measurement, Thermography.

## INTRODUCTION

The measurement of temperature in metal cutting has received much attention (Davies et al., 2007) as part of fundamental studies such as those concerned with tool-work material characterizations (Iraola et al., 2012), chip morphology (Gao et al., 2013) and tool wear and cut surface integrity (Jawahir et al., 2011). Infra-red microscopy (thermal imaging) is a well-established experimental method for observing and measuring cutting tool temperatures near the cutting edge, usually in orthogonal cutting. Figure 1 shows schematically a typical experimental arrangement. As a result of orthogonal machining, a tool makes contact with a chip (not shown) over a rectangle of width equal to  $a_p$  (the depth of cut) and height  $l_c$  (the chip / tool contact length). Heat flows into the tool through this contact area. The side face of the tool, heated by the machining, is specially prepared to be smooth and perpendicular to the cutting edge. The figure shows qualitatively a typical temperature distribution on the side face.

An infra-red camera is focussed on the side face. Much has been written about uncertainties in converting the image taken by the camera to a temperature map (Davies et al., 2007). At typical tool temperatures in general manufacturing machining (500 - 1000°C), uncertainties in camera calibration and emissivity of the cutting tool material lead to uncertainties in temperature values of around  $\pm 5\%$ .

However in all practical set-ups, the tool must overhang the chip / tool contact region by some distance  $d$ . This is required to avoid the chip flowing into the gap between the tool and camera. As a result the thermal image obtained by the camera is not from the edge of the contact. It is easily imagined that the larger is  $d$ , the lower will be the observed temperature. The systematic

error introduced by ignoring this offset in determining the temperature at the contact area has received little attention and is the subject of this note.

An approximate analytical model is developed for the temperature at the cutting edge of the side face when it is offset a distance  $d$  from the contact area. The model is at a similar level to classical theories of heating in cutting, for example (Shaw, 1984). The predictions are compared with existing but unpublished experimental measurements in the authors' possession. It is concluded that in typical set-ups, ignoring the offset may result in temperatures being underestimated by  $\approx 30\%$  or more.

## THEORY

Figure 2a shows the plan view of the rake face. The chip / tool contact area is assumed to be a rectangle of area  $l_c \times a_p$ , where  $l_c$  is the chip / tool contact length and  $a_p$  is the depth of cut. Heat flow from the chip to the tool is approximated as uniform over the contact area, with a flux  $q$  per unit area per unit time. It is required to estimate the temperature on the cutting edge at the point X on the side face of the tool, a distance  $d$  from the edge of the contact area.

Following the principle described by (Shaw, 1984), this temperature can be derived from the temperature at the surface of a semi-infinite solid heated over a rectangular area  $2l \times a_p$  by the heat flux  $q$ . Figure 2b shows such a source existing over the area  $-m < x < +m$  and  $-l < y < +l$  on the surface of the solid, where  $2m \equiv a_p$  and  $2l \equiv l_c$ . Figure 2c shows two sources each identical to that of Figure 2b, separated along the  $x$ -axis by  $2d$ . From symmetry there is no heat flow from one

quadrant to another. By inspection, the geometry of Figure 2a is reproduced in the top left-hand quadrant of Figure 2c. Then the temperature at X is obtained by the method of images, by superposition of the temperatures from each of the two sources.

It is a standard result for the case of Figure 2b that the steady state temperature rise  $\Delta T$  along the  $x$ -axis ( $y = 0$ ) is given by equation 1, with  $K$  the thermal conductivity of the solid (Shaw, 1984).

$$\Delta T = \frac{q}{\pi K} \left[ |x + m| \sinh^{-1} \left( \frac{l}{x + m} \right) - |x - m| \sinh^{-1} \left( \frac{l}{x - m} \right) + l \sinh^{-1} \left( \frac{x + m}{l} \right) - l \sinh^{-1} \left( \frac{x - m}{l} \right) \right] \quad (1)$$

In the case of Figure 2c, with two heat sources, the temperature rise at X is twice that given by equation 1. With axes centred in the left-hand heat source, X is at  $x = (0.5a_p + d)$ . Noting that in plane strain conditions  $l/(x + m) \ll 1$  so that in equation 1 the first term in the square bracket  $\approx l$ , and also substituting  $l = l_c$ ,  $m = 0.5a_p$ , leads to equation 2 for the temperature rise.

$$\Delta T = \frac{2q}{\pi K} l_c \left[ 1 - \frac{d/a_p}{l_c/a_p} \sinh^{-1} \left( \frac{l_c/a_p}{d/a_p} \right) + \sinh^{-1} \left( \frac{d/a_p + 1}{l_c/a_p} \right) - \sinh^{-1} \left( \frac{d/a_p}{l_c/a_p} \right) \right] \quad (2)$$

Figure 3a is a general view of the dependence of  $\Delta T$  on  $d/a_p$ , for a range of values of  $l_c/a_p$ . Figure 3b is a magnified view for  $0 < d/a_p < 0.4$ . In practice,  $l_c$  is fixed for any chosen value of uncut chip thickness and cutting speed.  $a_p$  and  $d$  are the experimental variables. Measuring the variation

of  $\Delta T$  with  $d$  at constant  $a_p$  and matching the results to those predicted by Figure 3 (or equation 2) may give a way of extrapolating to  $d = 0$ .

## **EXPERIMENTAL OBSERVATIONS AND DISCUSSION**

Figure 1's schematic arrangement has been realised in practice in orthogonal cutting, reducing the length of a tube rotating in the spindle of a high speed machining centre. The experimental equipment has been described elsewhere (Armendia et al., 2010a) with some details of the temperature calibration in this paper and also in (Arrazola et al., 2008).

The results from three sets of experiments are reported in this note. In the first one, Ti5Al4V (Ti54M, as forged, 237HB) was turned at  $v_c = 80$  m/min and uncut chip thickness (feed)  $h = 0.1$  mm by an uncoated carbide tool, rake angle  $7^\circ$ . The tube wall thickness was kept constant:  $a_p = 2$  mm.  $d$  was varied from 0.13 to 0.9 mm. The second was identical to the first ( $a_p = 2$  mm,  $d$  varied from 0.13 to 0.9 mm) except that AISI 4140 steel (tempered martensite, 290 HB) was turned at a cutting speed  $v_c = 250$  m/min and with  $h = 0.2$  mm by an alumina-coated carbide tool, rake angle  $5^\circ$ . In the third Ti6Al4V (Ti64, mill annealed HB240) was turned at  $v_c = 80$  m/min and  $h = 0.1$  mm also by an uncoated carbide tool, rake angle  $7^\circ$  but  $d$  was kept constant = 0.3 mm. Three wall thicknesses were used:  $a_p = 1, 1.5, 2$  mm. All experiments were carried out without cutting fluid.

Results are shown in Figure 4 compared to predictions from equation 2. Cutting and feed forces for these materials, and to a certain extent chip thicknesses too, have been reported previously (Armendia et al., 2010a,b; Arrazola et al., 2009).

The effect of varying  $d$  is shown in Figure 4a. For Ti54M, experimental observations are compared to the model predictions for  $l_c/a_p = 0.05, 0.1, 0.2$ . These predictions span the experimental results. In order to fit experimental results with theory predictions (equation 2), it is necessary to estimate  $l_c$ . Split tool tests show that  $l_c$  commonly is between one and two times the chip thickness, with the friction heat source fraction of the contact predominantly within one times the chip thickness (Childs et al., 2000). In this work it is assumed that  $l_c$  equals chip thickness, therefore, while chip thickness for Ti54M  $\approx h$  (Armendia et al., 2010b),  $l_c/a_p \approx 0.05$  in the present case. The theory marginally overestimates the observed variation of  $\Delta T$  with  $d$ , specially for small values ( $d < 0.13$ ). For AISI 4140, chip thickness  $\approx 2h$  (Armendia et al., 2010a). Then, in the present case,  $l_c/a_p \approx 0.2$ . Theory and experiment are in agreement.

The predicted values have been scaled to match the experimental values at  $d = 0.13$  mm. To achieve this for Ti54M ( $ql_c/K$ ) has been given the value  $415 \text{ }^\circ\text{C}^{-1}$  for  $l_c/a_p = 0.05$ ,  $445 \text{ }^\circ\text{C}^{-1}$  for  $l_c/a_p = 0.1$  and  $480 \text{ }^\circ\text{C}^{-1}$  for  $l_c/a_p = 0.2$ . For  $l_c = 0.1$  mm and supposing  $K = 50 \text{ W/mK}$ ,  $q$  is then  $\approx 200$  to  $240 \text{ MW/m}^2$ . The chip / tool friction force  $\approx 350 \text{ N}$  for  $a_p = 2 \text{ mm}$  (Armendia et al., 2010b). For  $l_c = 0.1$  mm and chip thickness =  $h$ , so that chip speed is equal to the cutting speed, the chip / tool friction heating rate is  $\approx 2.4 \text{ GW/m}^2$ . These calculations give 7 to 10% of the friction heat flowing into the tool. For AISI 4140, ( $ql_c/K$ ) =  $670 \text{ }^\circ\text{C}^{-1}$  for  $l_c/a_p = 0.2$ . For  $l_c = 0.4$  mm and also supposing  $K = 50 \text{ W/mK}$ ,  $q$  is then  $\approx 80 \text{ MW/m}^2$ . The chip / tool friction force  $\approx 300 \text{ N}$  for  $a_p = 2 \text{ mm}$

(Arrazola et al., 2009). For  $l_c = 0.4$  mm and chip thickness  $=2h$ , so that chip speed is equal to half the cutting speed, the chip / tool friction heating rate is  $\approx 800$  MW/m<sup>2</sup>. This gives 10% of the friction heat flowing into the tool. These % values are as expected from classical heat conduction theory for the present speed and feed conditions (Childs et al., 2000). The matching of theory with experiments, with realistic input data to the theory, approximately validates Equation 2.

The temperature variation with  $a_p$  (Figure 4b) does not follow theory. Although tool temperature rise decreases with reducing  $a_p$  for both theory and experiment, the experimental rate of reduction is less than the theoretical one. In this case theory and experiment have been matched at  $a_p = 2.0$  mm. Chip thickness is known to be approximately  $1.3h$  (Armendia et al., 2010b), therefore, taking into account the assumption that  $l_c$  equals chip thickness,  $l_c = 1.3h$  too, and  $l_c/a_p = 0.065$  when  $a_p = 2$  mm. It increases to 0.13 as  $a_p$  reduces to 1 mm. However, the discrepancy between theory and experiment is found not to be sensitive to the choice of  $l_c/a_p$ , but only to its change, and that of  $d/a_p$ , with reducing  $a_p$ .

Although theory and experiment do not agree in all respects, the similarities are such that the implication of Figure 4a cannot be ignored. Even with  $d$  at its practical minimum value ( $\approx 0.1$  mm), the observed cutting edge temperature rise may be severely underestimated. In the present examples the underestimates are  $\approx 250^\circ\text{C}$  in  $750^\circ\text{C}$  (Ti54M) or  $850^\circ\text{C}$  (AISI 42140), or  $\approx 30\%$ . Such a systematic error is much larger than calibration uncertainties of  $\pm 5\%$ . These example observations support the need for a more detailed numerical study of the influence of tool overhang on tool temperatures determined by the present experimental method.

## **CONCLUSION**

When chip / tool contact temperatures are estimated by observing the temperature distribution on a side face of the tool away from the contact there is in principle a systematic error arising from ignoring the distance of the side face from the contact. This short communication presents an approximate analysis of heat conduction in a tool that predicts how temperature on a side face reduces with distance from the contact and applies it to the authors' existing results from a well-established experimental technique, namely infra-red microscopy. It shows that cutting edge temperatures deduced from the technique's observations may be systematically underestimated by at least  $\approx 30\%$  if the offset distance is ignored, as is commonly the case. This is a large and systematic error compared to the  $\pm 5\%$  that is accepted as the uncertainty due to camera calibration and emissivity variability. There is a need for a more comprehensive study to support the interpretation of experimental measurements.

## **ACKNOWLEDGMENTS**

The authors thank the Basque and Spanish Governments for the financial support given to the projects INPRORET (code IE12-342), INPRORET II (code IE13-365), METINCOX (codes PI2010–11 and DPI2009-14286-C02-01).

## **REFERENCES**

Armendia, M.; Garay, A.; Villar, A.; Davies, M.A.; Arrazola, P.J. (2010a) High bandwidth temperature measurement in interrupted cutting of difficult to machine materials. *Annals CIRP* 59/1: 97-100.

Armendia, M.; Garay, Iriarte, L.M.; Arrazola, P.J. (2010b) Comparison of the machinabilities of Ti6Al4V and Timetal 54M using uncoated WC-Co tools. *Journal of Materials Processing Technology*, 210:197 – 203.

Arrazola, P.J.; Arriola A.; Davies, M.A.; Cooke, A.L., Dutterer, B.S. (2008) The effect of machinability on thermal fields in orthogonal cutting AISI 4140 steel. *Annals CIRP* 57/1: 65-68.

Arrazola, P.J.; Arriola, I.; Davies, M.A. (2009) Analysis of influence of tool type, coatings and machinability on the thermal fields in orthogonal machining of AISI 4140 steels. *CIRP Annals* 58/1: 85-88.

Childs, T.H.C.; Maekawa, K.; Obikawa, T.; Yamane, Y. (2000) *Metal Machining Theory and Applications*. Arnold: London: Section 2.3.2, and 2.4.1.

Davies, M.A; Ueda, T.; M'Saoubi, R.; Mullany, B.; Cooke, A.L. (2007) On the measurement of temperature in material removal processes. *CIRP Annals* 56/2: 581-604.

Gao, Chongyang, and Liangchi Zhang. "Effect of cutting conditions on the serrated chip formation in high-speed cutting." *Machining Science and Technology* 17.1 (2013): 26-40.

Iraola, J., et al. "Characterization of friction coefficient and heat partition coefficient between an austenitic steel aisi304l and a tin-coated carbide cutting tool." *Machining Science and Technology* 16.2 (2012): 189-204.

Jawahir IS, Brinksmeier E, M'Saoubi R, Aspinwall DK, Outeiro JC, Meyer D, Umbrello D, Jayal AD (2011) Surface integrity in material removal processes: recent advances. *CIRP Annals* 60/2:603-626.

Shaw, M.C. (1984). *Metal Cutting Principles*. Clarendon Press: Oxford: Ch. 12.

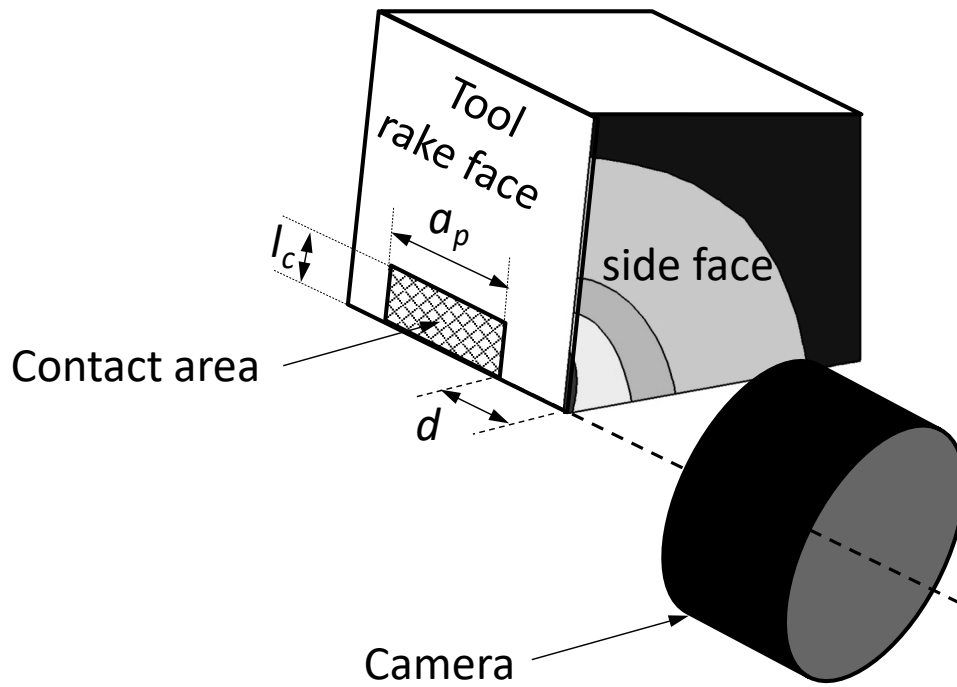


Figure 1. Schematic view of tool and camera for infra-red photography of tool side face.

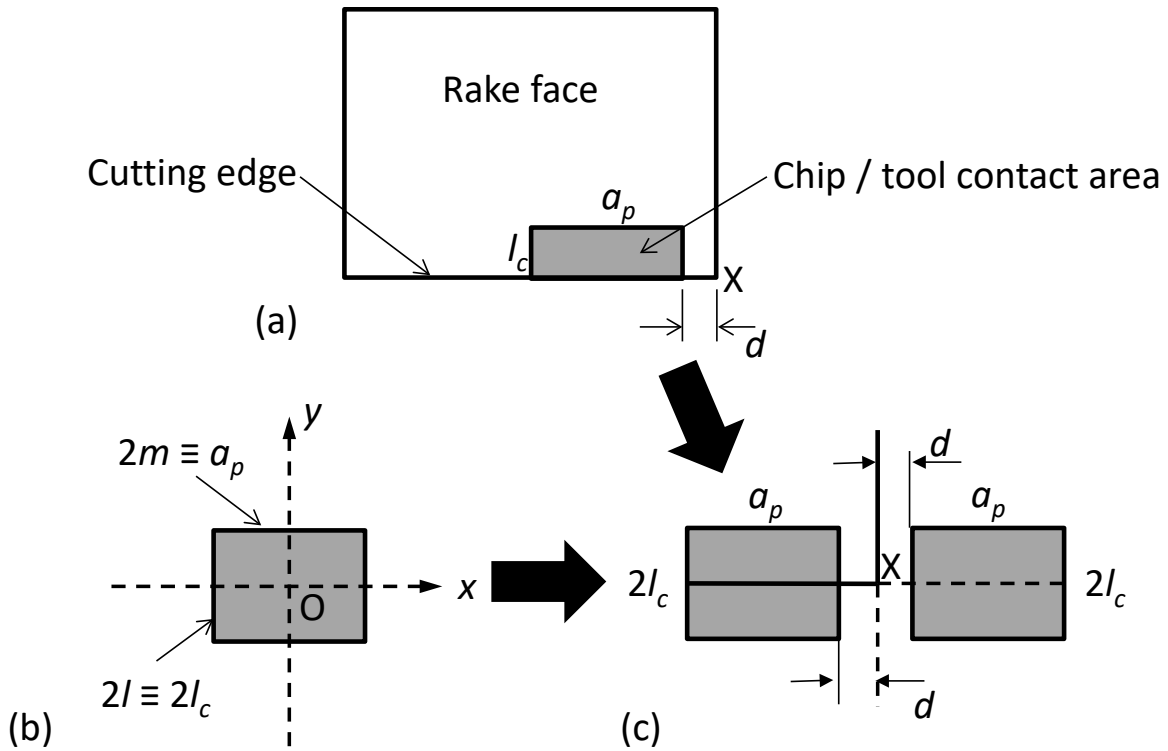


Figure 2. (a) Plan view of the rake face; (b) a rectangular heat source on the surface of a semi-infinite solid; (c) the heat source of (b) duplicated by the method of images to give the geometry of (a) in its upper left-hand quadrant.

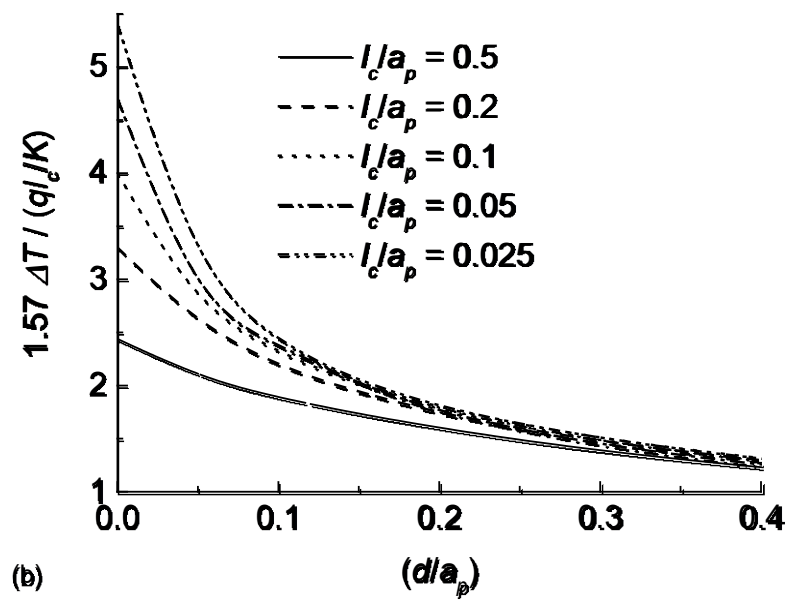
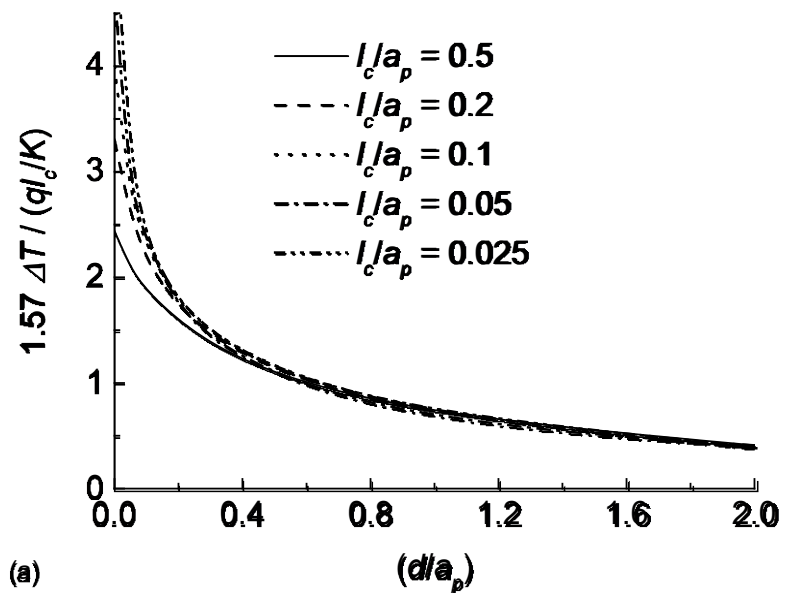


Figure 3. Predicted dependence of temperature rise at X on  $d/a_p$  and  $l_c/a_p$ : (a) a general and (b) a detail view.

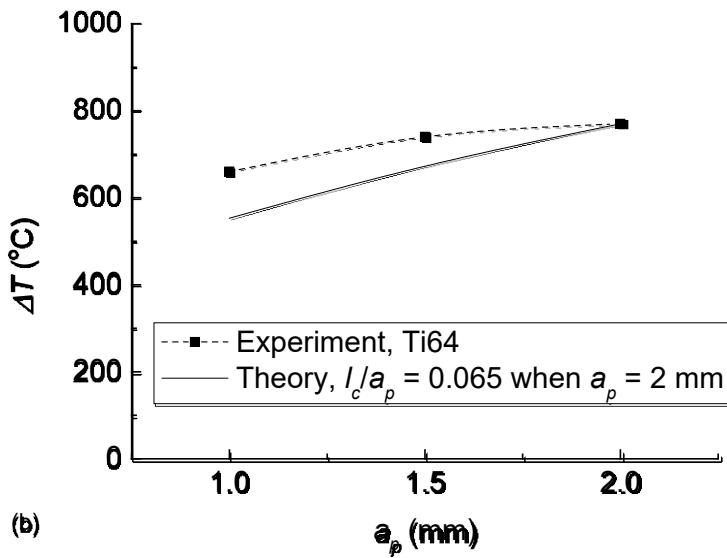
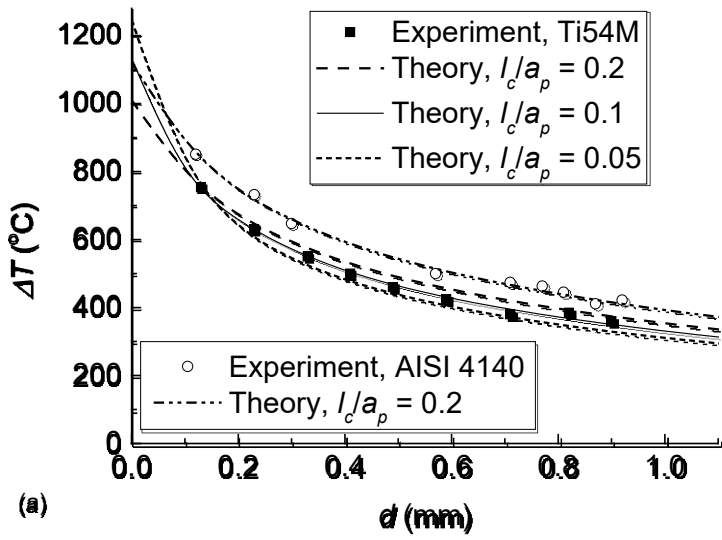


Figure 4. Experimental and theoretical comparisons: (a)  $d$  varying at constant  $a_p = 2\text{mm}$ :  $h/a_p = 0.05$  (Ti54M),  $0.1$  (AISI 4140) (b)  $a_p$  varying at constant  $d = 0.3\text{ mm}$ :  $h/a_p = 0.05$  to  $0.1$